QCD AT HIGH TEMPERATURES AND FINITE DENSITIES: HEAVY-ION COLLISIONS*

Federica Fabiano

on behalf of the LHCb Collaboration

Università degli Studi di Cagliari, Cagliari, Italy
and
INFN Sezione di Cagliari, Cagliari, Italy
federica.fabiano@cern.ch

Received 13 February 2023, accepted 24 August 2023, published online 27 October 2023

The LHCb Collaboration pursues a full physics program studying dense QCD with both beam–beam and fixed-target collisions. In this contribution, we present the recent LHCb results including quarkonia production in peripheral and ultra-peripheral heavy-ion (HI) collisions, antiproton, and charm production in fixed-target collisions.

DOI:10.5506/APhysPolBSupp.16.8-A11

1. Introduction

The LHCb detector is a single-arm forward spectrometer with a unique coverage in pseudorapidity, $2 < \eta < 5$, with respect to other LHC experiments [1, 2]. The detector includes a high-precision tracking system providing optimal vertex and momentum resolution, two ring-imaging Cherenkov detectors for charged particle identification, a calorimeter system to identify photons, electrons and hadrons, and a muon system. The LHCb fixed-target system, called SMOG (System for Measuring the Overlap with Gas), allows for injecting a low flow rate of noble gas into the primary LHC vacuum, and studying beam–gas collisions at different nucleon–nucleon centre-of-mass (c.m.) energies, $\sqrt{s_{NN}}$.

The LHCb has collected a wide variety of HI and fixed-target data in recent years. In the standard collision mode, lead–lead (PbPb) data have been acquired at $\sqrt{s_{NN}} = 5.02$ TeV with 60–100% centrality range in the LHC Run 2 (2015–2018), limited by the hardware saturation due to the high track density in the forward region. In the fixed-target configuration,

* Presented at *Excited QCD 2022*, Sicily, Italy, 23–29 October, 2022.

several samples of beam–gas collisions were acquired from 2015 to 2018 at $\sqrt{s_{NN}} = 69$, 110 GeV. These energies are higher compared to previous fixed-target experiments, but below the top RHIC energy for AA collisions.

2. PbPb collisions results

2.1. Λ_c^+-to-D^0 production cross-section ratio in peripheral PbPb collisions

Heavy flavour hadrons are an optimal tool to study hadronization, in particular with baryon-to-meson production ratios. The hadronization of the c-quark has been studied here, considering the Λ_c^+-to-D^0 ratio in peripheral PbPb collisions at $\sqrt{s_{NN}} = 5.02$ TeV [3]. The two particles have been reconstructed via the $\Lambda_c^+ \to pK^-\pi^+$ and $D^0 \to K^-\pi^+$ decay processes. The results for the Λ_c^+-to-D^0 cross-section ratio are reported as a function of the transverse momentum in Fig. 1 and compared both to theoretical models (left) and to a previous pPb LHCb measurement at $\sqrt{s_{NN}} = 5.02$ TeV (right) [4]. Considering the colour recombination mechanism, data are sufficiently well described by the model except at $p_T < 3$ GeV, while a disagreement is found with the statistical hadronization theory. The measurement with PbPb data shows no dependence on the number of participants, but points toward a strong dependence of R_{Λ_c/D^0} with rapidity.

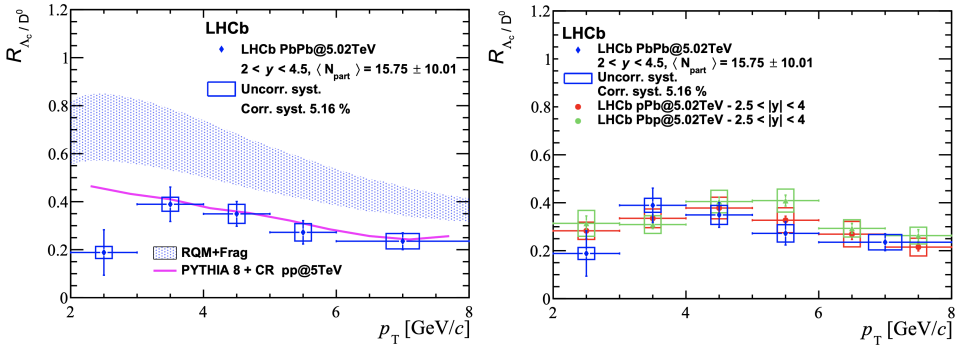


Fig. 1. Measurement of the Λ_c^+-to-D^0 ratio as a function of p_T compared to theoretical models (left) and to a previous LHCb measurement with pPb data (right).

2.2. Coherent charmonium production in ultra-peripheral lead–lead collisions

In ultra-peripheral collisions (UPCs), the two ions interact via a photon-nuclear process. If the photon interacts with the whole nucleus coherently, this process is a great tool to constrain the gluon parton distribution function (PDF). Hence, the coherent J/ψ and $\psi(2S)$ production cross sections in PbPb UPCs at $\sqrt{s_{NN}} = 5.02$ TeV are studied as a function of p_T [5].

Once the particles are reconstructed, the differential cross sections are separately measured for J/ψ and $\psi(2S)$ as a function of the rapidity and the transverse momentum in the c.m. system in the ranges of $2.0 < y^* < 4.5$ and $0 < p_{\rm T}^* < 0.2$ GeV/c, respectively. The ratio of cross sections between the coherent $\psi(2S)$ and J/ψ yields as a function of y^* is precisely determined for the first time in PbPb collisions at the LHC, finding compatibility with theoretical models.

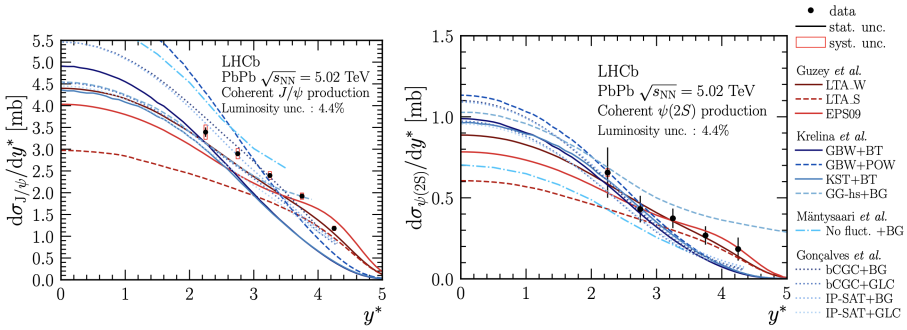


Fig. 2. (Colour on-line) Differential cross section as a function of y^* for coherent J/ψ (left) and $\psi(2S)$ (right) production, compared to theoretical predictions. Models are grouped as perturbative QCD (red lines) calculations and colour glass condensate (blue lines).

3. Fixed-target collisions results

3.1. $\bar{p}$ production from antihyperon decays in pHe collisions at $\sqrt{s_{NN}} = 110$ GeV

The LHCb fixed-target programme is also relevant to cosmic ray physics, *e.g.* to constrain the flux of antiprotons in space originating in cosmic rays spallation on the interstellar medium, mainly composed of hydrogen and helium. The antiproton production has been measured in the pHe sample at $\sqrt{s_{NN}} = 110$ GeV, an energy scale relevant for the AMS-02 measurements of antimatter in space [6, 7]. Prompt $\bar{p}$ measurements already constrained models of secondary cosmic antiprotons [8]. Thus, searches are now extended to antiprotons produced by antihyperons decays performed with two complementary approaches: *(i)* inclusive measurements of detached antiprotons using impact parameter and $\bar{p}$ identification; *(ii)* exclusive measurements of the dominant contribution $\bar{\Lambda} \to \bar{p}\pi^+$. Despite that the most commonly used hadronic models underestimate the antihyperon contributions to the total yield (Fig. 3 (left)), an agreement of the exclusive $\bar{\Lambda}$ over inclusive antihyperon ratio $R_{\bar{\Lambda}/\bar{H}}$ with theoretical expectations can be found (Fig. 3 (right)).

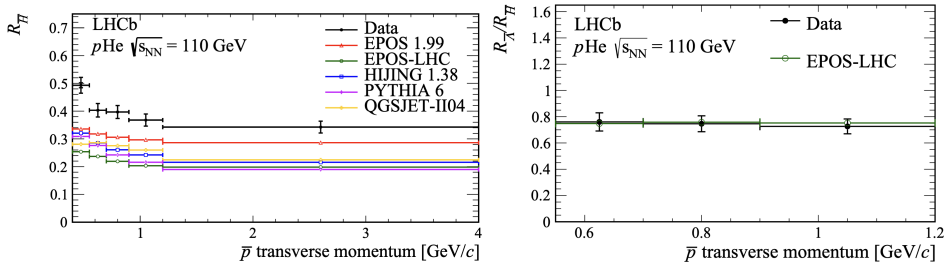


Fig. 3. Measurement of $R_{\bar{H}}$ ratio as a function of the transverse momentum compared to theoretical predictions (left); detached-to-prompt $\bar{\Lambda}$-to-$\bar{H}$ ratio with the EPOS-LHC prediction (right).

3.2. Charmonium production in pNe collisions at $\sqrt{s_{NN}} = 68.5$ GeV

Charmonia production is an excellent probe for Cold Nuclear Matter effects such as PDF nuclear modification, nuclear absorption, multiple scatterings, *etc.* The production of J/ψ and $\psi(2S)$ mesons reported here is studied with 2.5 TeV protons colliding on gaseous neon targets at rest, corresponding to $\sqrt{s_{NN}} = 68.5$ GeV [9]. The J/ψ differential cross section is in good agreement with predictions with and without 1% intrinsic charm contribution, while there is tension between data and HELAC-ONIA model (Fig. 4 (left)) [10]. This is the first measurement of the $\psi(2S)$-to-J/ψ production ratio with SMOG, and it is consistent with other pA measurements at small atomic mass number A (Fig. 4 (right)), but with limited statistics. This suggests and motivates the fixed-target programme upgrade.

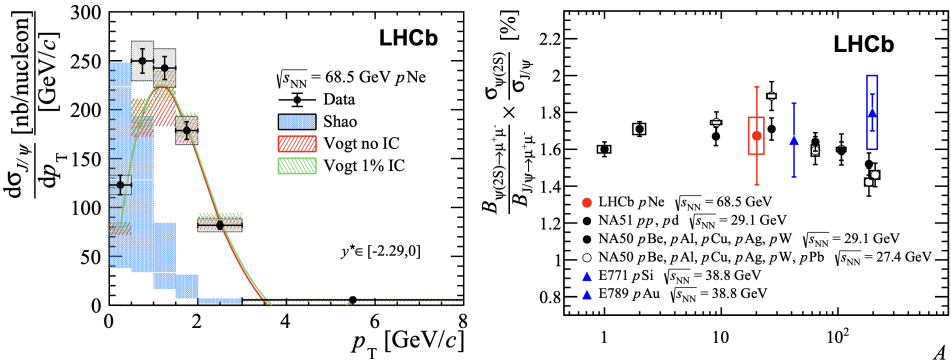


Fig. 4. (Colour on-line) Differential J/ψ cross section as a function of p_T (left). Blue boxes correspond to HELAC-ONIA predictions. Green and red boxes correspond to predictions (Vogt) with and without a 1% intrinsic charm contribution, respectively. The $\psi(2S)$-to-J/ψ production ratio as a function of the target atomic mass number A (right).

3.3. J/ψ and D^0 production in PbNe collisions at $\sqrt{s_{NN}} = 68.5$ GeV

At larger values compared to the QGP critical temperature (~ 156 MeV), lattice QCD predicts the charmonium production decrease with respect to the overall $c\bar{c}$ production, due to the modification of their binding mechanism [10]. Consequently, since most of the charm quarks hadronize into open charm mesons, the D^0 production yield provides a suitable reference for the study of the charmonium yield modification when traversing nuclear media. The production of J/ψ and D^0 mesons is studied for the first time with a beam of lead ions with an energy of 2.5 TeV per nucleon colliding on gaseous neon targets at rest, corresponding to a nucleon–nucleon c.m. energy of $\sqrt{s_{NN}} = 68.5$ GeV [11]. The J/ψ over D^0 production cross section is computed as a function of rapidity, transverse momentum, and collision centrality. A decrease of J/ψ over D^0 ratio with increasing centrality has been observed, in agreement with NA50-SPS pA measurements (Fig. 5 (left)) [12]. Hence, these data are compared with measurements from pNe collisions at the same energy. No anomalous J/ψ suppression that could indicate the formation of a deconfined medium is observed (Fig. 5 (right)).

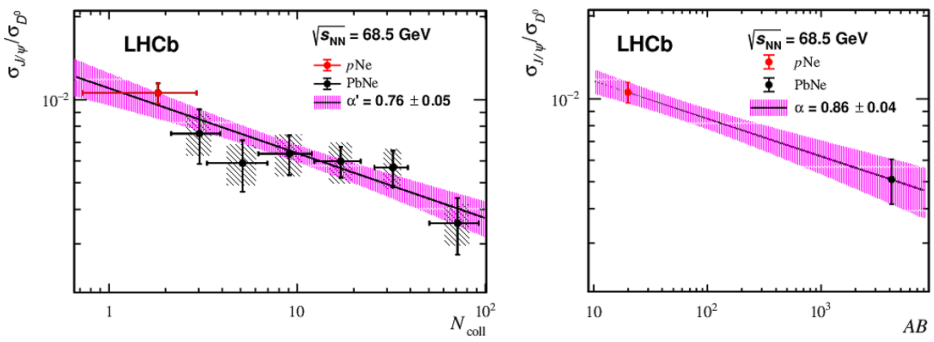


Fig. 5. (Colour on-line) Left: $J/\psi/D^0$ cross-section ratio as a function of the number of binary collisions, $N_{\rm coll}$. The red and black points correspond to pNe and PbNe collisions, respectively. Right: $J/\psi/D^0$ cross-section ratio as a function of AB, the product of the beam (A) and target (B) atomic mass numbers.

4. Run 3 performance: the LHCb upgrade

The LHCb has undergone a major upgrade in 2018–2022 to meet the challenge of the increased luminosity in the LHC Run 3 [13]. The upgrade will reduce the occupancy limitation in PbPb collisions and allow for access to mid-central PbPb collisions up to 30% in centrality (Fig. 6 (left)). The other significant improvement is the new fixed-target storage cell located upstream of the LHCb interaction point, SMOG2 (Fig. 6 (right)). This new

configuration allows for the injection of heavier noble gases (Kr, Xe) and non-noble species (H_2, D_2, O_2, N_2) with a pressure of about two orders of magnitude higher than the SMOG one for the same gas flow, leading to higher luminosities for fixed-target collisions [14].

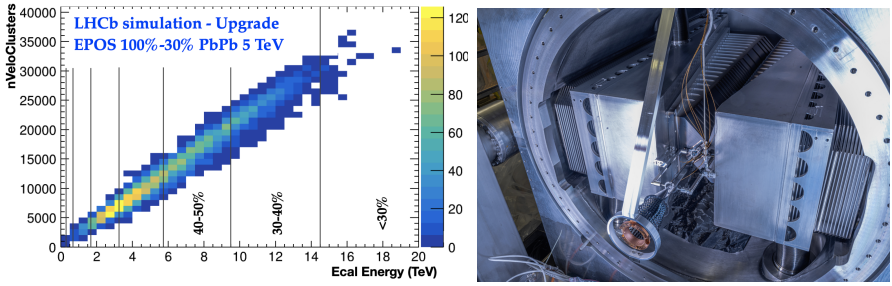


Fig. 6. Left: Reconstruction performance in LHCb Run 3 for Pb–Pb collisions. The nVeloClusters variable is related to the centrality. Right: SMOG2 storage cell.

5. Conclusions and outlook

The results presented here from PbPb datasets demonstrate the capabilities of LHCb in studying nuclear effects in different centrality regions. In addition, the fixed-target programme is relevant also to cosmic ray physics as well as nuclear matter effects and QGP formation.

With the upgrade, LHCb will be able to acquire PbPb and fixed-target data samples with increased statistics, opening the gates to more precise measurements and a wider variety of possible analyses. PbPb collisions up to mid-central events will enable QGP studies, and SMOG2 will bring the current fixed-target measurements to a new level.

REFERENCES

[1] LHCb Collaboration (A.A. Alves Jr. *et al.*), *J. Instrum.* **3**, S08005 (2008).

[2] LHCb Collaboration (R. Aaij *et al.*), *Int. J. Mod. Phys. A* **30**, 1530022 (2015), arXiv:1412.6352 [hep-ex].

[3] LHCb Collaboration (R. Aaij *et al.*), *J. High Energy Phys.* **2023**, 132 (2023), arXiv:2210.06939 [hep-ex].

[4] LHCb Collaboration (R. Aaij *et al.*), *J. High Energy Phys.* **2019**, 102 (2019), arXiv:1809.01404 [hep-ex].

[5] LHCb Collaboration (R. Aaij *et al.*), *J. High Energy Phys.* **2023**, 146 (2023), arXiv:2206.08221 [hep-ex].

[6] LHCb Collaboration (R. Aaij *et al.*), *Eur. Phys. J. C* **83**, 543 (2023), arXiv:2205.09009 [hep-ex].

[7] A. Kounine, *Int. J. Mod. Phys. E* **21**, 1230005 (2012).
[8] LHCb Collaboration (R. Aaij *et al.*), *Phys. Rev. Lett.* **121**, 222001 (2018).
[9] LHCb Collaboration (R. Aaij *et al.*), *Eur. Phys. J. C* **83**, 625 (2023), arXiv:2211.11645 [hep-ex].
[10] H.-S. Shao, *Comput. Phys. Commun.* **198**, 238 (2016), arXiv:1507.03435 [hep-ph].
[11] LHCb Collaboration (R. Aaij *et al.*), *Eur. Phys. J. C* **83**, 658 (2023), arXiv:2211.11652 [hep-ex].
[12] NA50 Collaboration (M.C. Abreu *et al.*), *Phys. Lett. B* **410**, 337 (1997).
[13] LHCb Collaboration, CERN-LHCC-2012-007; LHCb-TDR-012.
[14] LHCb Collaboration, LHCB-TDR-020.